

## RECENT SEARCH FOR NEW PARTICLES AT CELLO

R. ALEKSAN

Département de Physique des Particules Élémentaires, CEN-Saclay,  
91191 Gif-sur-Yvette Cedex, France.

## ABSTRACT

A search for a scalar particle decaying to  $e^+e^-$ ,  $\mu^+\mu^-$ ,  $\tau^+\tau^-$  or  $\gamma\gamma$  was done in  $e^+e^-$  collisions between 39.79 to 45.22 GeV c.m. using the CELLO detector at PETRA. No evidence for such new particle has been observed.

An event with 2 topologically isolated energetic muons of opposite charge and 2 hadronic jets has been observed. The masses of  $\mu^+\mu^-$ , jet-jet or  $\mu^+$  + jet combination are large, leading to an expected number for such events from known processes of the order of  $10^{-5}$ . Non conventional sources are also discussed.

## Introduction

The  $e^+e^-$  interactions are a very appropriate tool for the search of new particles. A search for a scalar boson was done with the CELLO detector. In addition, while looking for isolated energetic muons, an unusual multihadronic event with 2 energetic muons was observed.

## Data and experimental set up.

The data were taken in 1983 with the CELLO detector at PETRA during a scan in energy between 39.79 GeV and 45.22 GeV. The energy steps were 30 MeV in c.m. which is the energy resolution of PETRA and the total integrated luminosity was  $8 \text{ pb}^{-1}$ .

CELLO [1] is a general purpose detector for  $e^+e^-$  physics. Interleaved cylindrical drift and proportional chambers, in a 13 kG magnetic field produced by a thin superconducting solenoid, measure charged particle momenta over 92% of the solid angle with a resolution of  $.013 \sqrt{1+p_T^2}$ .  $p_T$  ( $p_T$  in GeV/c). A lead-liquid Argon calorimeter covering a solid angle of 86 % of  $4\pi$  steradians gives an energy resolution of  $\sigma(E)/E = .13/\sqrt{E}$  for electromagnetic showers. Large planar drift chambers mounted on a hadron absorber of 80 cm thick iron ensure muon identification over 92 % of  $4\pi$  steradians.

## I - Search for scalar bosons.

### 1) Motivation

The observation at the CERN  $p\bar{p}$  collider of radiative decays of the neutral vector boson  $Z^0$  [2] with a rate higher than the one expected from the bremsstrahlung process [3] might have an explanation through composite models [4]. Among the different possible mechanisms using composite objects, we concentrate on the transition via a scalar or/and pseudoscalar boson.

$$Z^0 \rightarrow X \gamma, \quad X \rightarrow f\bar{f}, \gamma\gamma \quad (1)$$

These spinless particles X would have to be in a parity doublet in order to conserve the chiral symmetry and preserve composite fermions from acquiring a mass of order  $M_{W,Z}$  [5].

The two  $Z \rightarrow e^+e^- \gamma$  events seen at the collider when 12  $Z \rightarrow e^+e^-$  events are observed suggest :

$$\Gamma(Z \rightarrow X\gamma) \cdot \text{Br}(X \rightarrow e^+e^-) \simeq 15 \text{ MeV} \quad (2)$$

Because of the leptonic coupling, such objects could be produced in  $e^+e^-$  collisions. Making use of VDM (vector dominance),  $\Gamma(Z \rightarrow X\gamma)$  can be expressed in terms of  $\Gamma(X \rightarrow \gamma\gamma)$  [6].

$$\frac{\Gamma(X \rightarrow \gamma\gamma)}{\Gamma(Z \rightarrow X\gamma)} = \frac{3}{2} \sin^2 \theta_W \left[ \frac{M_Z}{M_X} - \frac{M_X}{M_Z} \right]^{-3} = \rho_{\text{VDM}} \quad (3)$$

and therefore (noting  $\Gamma_{ii} = \Gamma(X \rightarrow ii)$ )

$$\Gamma_R = \Gamma(Z \rightarrow ee\gamma) = \frac{\epsilon \Gamma_{ee} \Gamma_{\gamma\gamma}}{\rho_{\text{VDM}} \Gamma_X} \quad (4)$$

where  $\epsilon = 1, 2$  depending on the number of spin 0 bosons contributing.

Since  $\text{Br}(X \rightarrow \gamma\gamma) \leq 1$ , equation (4) leads to the lower bound :

$$\epsilon \Gamma_{ee} \geq \rho_{\text{VDM}} \Gamma_R \quad (5)$$

$$\text{where } \Gamma_{ee} = a_H M_X / 2 \quad (6)$$

$a_H$  is the coupling constant of the interactions between constituents [6].

A systematic search for the spin 0 boson was carried on at CELLO in the channels :

$$e^+e^- \rightarrow e^+e^- \quad (7)$$

$$e^+e^- \rightarrow \gamma\gamma \quad (8)$$

$$e^+e^- \rightarrow \mu^+\mu^- \quad (9)$$

$$e^+e^- \rightarrow \tau^+\tau^- \quad (10)$$

## 2) Results

The presence of scalar particles will contribute to all these channels by adding terms to the differential cross sections.

a) In  $e^+e^- \rightarrow e^+e^-$ , additional terms to those of the electroweak differential cross section are due to the interference between the scalar and the vector boson as well as an isotropic part purely due to the scalar boson [6,7].

$$\begin{aligned}
\left(\frac{d\sigma}{d\Omega}\right)_{e^+e^-} \sim & \frac{\alpha \epsilon \Gamma_{ee} s}{2M_X [(s-M_X^2)^2 + M_X^2 \Gamma_X^2]} \left[ \frac{2(s-M_X^2)}{t} + \frac{2\Gamma_{ee}}{M_X \alpha} \right] \\
& + \frac{\alpha \epsilon \Gamma_{ee} t^2}{2s M_X [(t-M_X^2)^2 + M_X^2 \Gamma_X^2]} \left[ \frac{2(t-M_X^2)}{s} + \frac{2\Gamma_{ee}}{M_X \alpha} \right] \\
& + (2-\epsilon) \frac{\epsilon \Gamma_{ee}^2}{s M_X^2 [(s-M_X^2)^2 + M_X^2 \Gamma_X^2]} \frac{t}{(t-M_X^2)^2 + M_X^2 \Gamma_X^2} [(s-M_X^2)(t-M_X^2) + M_X^2 \Gamma_X^2]
\end{aligned} \quad (11)$$

where  $\sqrt{s}$  = center of mass energy,  $t = -\frac{s}{2}(1-\cos\theta)$ ,  $M_X$  = the mass of the scalar boson. In the formula, contributions from  $X$ - $Z^0$  interference have been omitted since they are negligible.

b) In the other channels, only an isotopic term given by the usual Breit-Wigner has to be added:

$$\left(\frac{d\sigma}{d\Omega}\right)_{\gamma\gamma} = 2\left(\frac{s}{M_X^2}\right)^2 \frac{\epsilon \Gamma_{ee} \Gamma_{\gamma\gamma}}{[(s-M_X^2)^2 + M_X^2 \Gamma_X^2]} \quad (12)$$

or

$$\left(\frac{d\sigma}{d\Omega}\right)_{f\bar{f}} = \left(\frac{s}{M_X^2}\right)^2 \frac{\epsilon \Gamma_{ee} \Gamma_{f\bar{f}}}{[(s-M_X^2)^2 + M_X^2 \Gamma_X^2]} \quad (13)$$

We have first assumed that the scalar boson mass lies between 39.79 and 45.22 GeV/c<sup>2</sup> and searched for a resonant state. In the  $e^+e^-$  sample, a cut at  $\cos\theta < 0$  was made to increase the sensitivity to a spin 0 boson and this cut was set at  $|\cos\theta| < .65$  in the  $\gamma\gamma$  sample. For a total boson width smaller than the c.m. energy spread of PETRA, the experimental cross section is folded with the energy resolution function. No significant structure is observed in our data (fig.1) and the limits at 95% CL (confidence level) are listed in table 1.

	CELLO	MARK J
$\epsilon\Gamma_{ee} \text{Br}(X \rightarrow ee)$	$< 9.9 \text{ keV}$	
$\epsilon\Gamma_{ee} \text{Br}(X \rightarrow \mu\mu)$	$< 5.6 \text{ keV}$	$< 4.5 \text{ keV}$
$\epsilon\Gamma_{ee} \text{Br}(X \rightarrow \tau\tau)$	$< 7.0 \text{ keV}$	
$\epsilon\Gamma_{ee} \text{Br}(X \rightarrow q\bar{q})$	$< 8.1 \text{ keV (prel)}$	$< 8.7 \text{ keV}$
$\epsilon\Gamma_{ee} \text{Br}(X \rightarrow \gamma\gamma)$	$< 2.6 \text{ keV}$	$< 3.7 \text{ keV}$

Table 1

For  $M_X$  in the range of energies covered by the scan, one gets  $\epsilon\Gamma_{ee} \text{Br}(X \rightarrow \gamma\gamma) \geq 1 \text{ MeV}$  from equation (5). Such a value is clearly excluded from our results.

Assuming a broad resonance  $\Gamma_X M_X \gg s - M_X^2$ , one can derive limits in the same way (table 2).

	limit at 95% CL
$\epsilon\Gamma_{ee} \text{Br}(X \rightarrow e^+e^-)$	$< 3.9 \cdot 10^{-6} \Gamma_X$
$\epsilon\Gamma_{ee} \text{Br}(X \rightarrow \mu^+\mu^-)$	$< 3.0 \cdot 10^{-6} \Gamma_X$
$\epsilon\Gamma_{ee} \text{Br}(X \rightarrow \tau^+\tau^-)$	$< 6.5 \cdot 10^{-6} \Gamma_X$
$\epsilon\Gamma_{ee} \text{Br}(X \rightarrow \gamma\gamma)$	$< 2.2 \cdot 10^{-6} \Gamma_X$

Table 2

A resonance a few GeV broad is therefore excluded.

In case the mass of the scalar boson is greater than  $45.22 \text{ GeV}/c^2$ , a contribution in the channels discussed previously is still expected by the exchange of a virtual spin 0 boson. Fig.2 shows the limit obtained on the boson's partial widths using only the integrated cross sections.

However, better limits are achieved with the differential cross sections for reaction (7) and (8) as shown in fig.3 for  $e^+e^- \rightarrow e^+e^-$  (dashed line). In addition using equation (6) and assuming universality ( $\Gamma_X = 18\Gamma_{ee} + \Gamma_{\gamma\gamma}$ ), an allowed region of  $\alpha_H$  can be defined according to the mass of the scalar boson and for different values of the radiative width  $\Gamma_R$  (fig.3). Taking  $\Gamma_R = 15 \text{ MeV}$ , one is left with a narrow allowed region with our present data (shaded area in fig.3).

## II - Observation of a multihadronic event with 2 isolated energetic muons of opposite charge

A search for multihadronic events with isolated muons in our data at the highest energies (43.2 - 45.2 GeV c.m. corresponding to an integrated luminosity of  $3.9 \text{ pb}^{-1}$ ) has led to the finding of an unusual event with 2 topologically isolated energetic muons and 2 energetic jets of hadrons at a c.m. energy of 43.45 GeV.

### 1) Event description

A view in the plane perpendicular to the beam axis is shown in Fig.4a. The 2 muons, easily identified by the hits in the muon chambers, are very energetic ( $\geq 10 \text{ GeV/c}$ ) and well separated from other charged and neutral particles. Table 3a summarizes the values of muon and jet momenta.

(GeV)	E	$P_x$	$P_y$	$P_z$	M
$\mu^+$	11.0	- 7.0	8.5	.5	.105
$\mu^-$	12.6	11.0	1.3	- 6.1	.105
jet 1	10.1	- 7.4	- 4.2	4.8	2.4
jet 2	9.1	6.7	- 3.5	- 2.0	4.7

Table 3a - Muon and jet four-vectors

The event has a remarkably low aplanarity of  $A = \simeq .003$ . Fig.4b shows a momentum diagram in the plane defined by the 2 muons. The average  $\langle P_T \rangle$  relative to that plane is  $\langle |P_T^{\text{out}}| \rangle \simeq 270 \text{ MeV/c}$ . From Fig.4b, one can see that the event has the structure of 2 subsystems each containing a high momentum muon back to back to a jet. The invariant masses for all combinations  $\mu + \text{jet}$  are given in Table 3b.

Masses (GeV)	$\mu^+$	$\mu^-$	jet 1
jet 2	$19.4 \pm 1.3$	$9.5 \pm .5$	$17.3 \pm .3$
jet 1	$14.1 \pm 1.0$	$22.2 \pm 1.6$	
$\mu^-$	$20.4 \pm 1.1$		

Table 3b - Invariant masses

Sphericity and thrust values are respectively .36 and .86. The transverse momentum of the  $\mu^+$  relative to the thrust axis is 7.2 GeV/c and the nearest particle is at  $\cos\theta_{\min} \approx .47$ . The corresponding values for the  $\mu^-$  are 4.2 GeV/c and  $\cos\theta_{\min} \approx .97$ . Since almost all the c.m. energy is measured, we tried a 1-C fit accounting for the loss of a single light particle. A satisfactory solution was found with the following momentum vector :

$$P_X = -2.4 \pm .8, \quad P_Y = -1.1 \pm 1.2, \quad P_Z = 2.3 \pm .5 \text{ GeV/c.}$$

## 2) Study of conventional di-muon sources

$$a) e^+e^- \rightarrow q\bar{q}(g)$$

We have estimated the contribution of the semileptonic decays of heavy quarks and meson decays in flight as well as punch through and spurious association in the muon chambers due to background in the chambers. This study was done using the LUND event generator [8] where the Peterson fragmentation function [9] was used for heavy quarks and the branching ratio  $c \rightarrow \mu\nu_\mu + X$  and  $b \rightarrow \mu\nu_\mu + X$  were set to .09 and 0.12 respectively. Many checks on the multiplicities and prompt lepton momenta from B and D meson decays in their rest frame were done by comparing the event generator with DELCO and CLEO results [10]. Good agreement was also observed between the generator and our results [11] and that of TASSO [12] on the transverse momenta of leptons relative to the thrust axis. The expected number of events with 2 isolated energetic muons ( $P > 6 \text{ GeV/c}$ ) due to the semi-leptonic decays are given in brackets in Table 4 for different  $\cos\theta_{\min}$  values.

The charged multiplicities and momentum spectra of hadrons in the multihadronic events were well reproduced by our Monte Carlo. The same agreement was found for the  $\cos\theta_{\min}$  distribution of energetic hadrons ( $P \geq 4 \text{ GeV}$ ) at  $\sqrt{s} = 34 \text{ GeV}$  where our statistics is larger (fig.5). In the present data 22 events with isolated hadrons ( $P \geq 4 \text{ GeV/c}$ ,  $\cos\theta_{\min} \leq .8$ ) have been observed where 28 were expected according to the Monte Carlo. The ability of the program, which propagates the hadrons through the lead-liquid argon calorimeter and the hadron filter, to reproduce punch through correctly was checked by comparing its results for different absorber thicknesses with measurements [13]. Accounting for all the sources mentioned in this paragraph, we find an expected number of  $8.10^{-4}$  events in which 2 energetic muons ( $p > 10 \text{ GeV/c}$ ) are isolated from any other charged particles in a cone around their directions of 10 degrees. This number is still a conservative estimate since one of the muons has the nearest charged particle at  $\cos\theta_{\min} = .47$ . Table 4 shows the number of events expected for different  $\cos\theta_{\min}$  values and  $P_\mu > 6 \text{ GeV/c}$ .

$p > 6 \text{ GeV/c}$	$\cos\theta_{\min} < .98$	$\cos\theta_{\min} < .9$	$\cos\theta_{\min} < .8$	$\cos\theta_{\min} < .5$
$\cos\theta_{\min} < .98$	$2.7 \cdot 10^{-2}$ ( $2 \cdot 10^{-2}$ )			
$\cos\theta_{\min} < .9$	$1.6 \cdot 10^{-2}$ ( $1.3 \cdot 10^{-2}$ )	$6.1 \cdot 10^{-3}$ ( $5 \cdot 10^{-3}$ )		
$\cos\theta_{\min} < .8$	$4 \cdot 10^{-3}$ ( $2.5 \cdot 10^{-3}$ )	$1.8 \cdot 10^{-3}$ ( $1.6 \cdot 10^{-3}$ )	$< 8 \cdot 10^{-4}$ ( $< 8 \cdot 10^{-4}$ )	
$\cos\theta_{\min} < .5$	$< 8 \cdot 10^{-4}$ ( $< 8 \cdot 10^{-4}$ )	$< 8 \cdot 10^{-4}$ ( $< 8 \cdot 10^{-4}$ )	$< 8 \cdot 10^{-4}$ ( $< 8 \cdot 10^{-4}$ )	$< 8 \cdot 10^{-4}$ ( $< 8 \cdot 10^{-4}$ )

Table 4

$$b) e^+e^- \rightarrow \gamma^* \gamma^* \rightarrow \mu^+ \mu^- q\bar{q}$$

Several types of diagram are contributing at the  $\alpha^4$  order as shown in fig.6(a,b,c), each of which corresponds to 2 distinct graphs.

The factorisation of the cross section  $e^+e^- \rightarrow \mu^+ \mu^- \gamma$  up to a mass  $M_{\mu\mu} \approx \sqrt{s}/2$  into  $e^+e^- \rightarrow \gamma\gamma^*$  and  $\gamma^* \rightarrow \mu^+ \mu^-$  (where  $\gamma^*$  stands for a virtual photon of mass  $M_{\mu\mu}$ ) was found to be a good approximation [14] of the exact calculation [15]. By applying the same method to process (6a) and neglecting 6b,c we find :

$$\frac{d^3\sigma}{dM_{\mu\mu}^2 dM_{q\bar{q}}^2 d\cos\theta_{\gamma^*}} = \left(\frac{\alpha}{3\pi}\right)^2 \frac{R(M_{q\bar{q}}^2)}{M_{\mu\mu}^2 M_{q\bar{q}}^2} \frac{d\sigma}{d\cos\theta_{\gamma^*}}(M_{\mu\mu}, M_{q\bar{q}}) \quad (14)$$

where  $d\sigma/d\cos\theta_{\gamma^*}$  is the differential cross section for  $e^+e^- \rightarrow \gamma^* \gamma^*$  accounting for off shell photons.  $R(M_{q\bar{q}}^2)$  is the ratio of  $\sigma(ee \rightarrow \text{hadron})$  to  $\sigma(ee \rightarrow \mu\mu)$  at  $s = M_{q\bar{q}}^2$ . We have checked the result of our approximation with the result of a recent calculation by Kleiss [17] for  $e^+e^- \rightarrow \mu^+ \mu^- \ell^+ \ell^-$  using all graphs. At  $\sqrt{s} = 30 \text{ GeV}$ , for  $M_{\mu\mu}, M_{\ell\ell} > 1 \text{ GeV/c}$  and  $45^\circ < \theta_{\mu}, \theta_{\ell} < 135^\circ$ , we obtain a cross section of  $(6.8 \pm .3) \cdot 10^{-3} \text{ pb}$  whereas Kleiss obtains  $(8.2 \pm .5) \cdot 10^{-3} \text{ pb}$ . Using expression (14) and a full MC simulation of  $q\bar{q}$  jets, we have estimated the expected number of events for  $M_{\mu\mu}, M_{q\bar{q}} > 5 \text{ GeV}$ . (fig.7). The probability to observe one event of this process with  $\mu\mu$  and  $q\bar{q}$  masses equal or greater than the observed ones is less than  $(3.2 \pm 1.0) \cdot 10^{-4}$ .



c) Discussion on non-conventional di-muon sources.

a) New heavy quarks

The production of new heavy quarks could produce muons with high  $P_T$  relative to the event thrust axis. During our energy scan, no narrow resonance nor a step in  $R$  with  $\Delta R = 1.3$ , (where  $R$  is  $\sigma(e^+e^- \rightarrow q\bar{q})/\sigma(e^+e^- \rightarrow \mu^+\mu^-)$ ) were observed. Therefore the production of a charge  $2/3$  quark is ruled out. However the continuum production of a charge  $1/3$  quark is not excluded though missing energy and momentum from neutrinos is expected to be greater than observed.

$\beta$ ) Heavy charged new particles

Spin 0 Higgs-like charged particles  $H^\pm$ , couple preferentially to heavy fermions ( $\nu_\tau, \tau, c\bar{s}, c\bar{b}$ ). When both  $H^\pm$  decay into quarks, isolated energetic muons are unlikely. One isolated muon can be obtained when one of the Higgs particles decays into  $\nu_\tau, \tau$ . However substantial energy carried out by neutrinos should be missing. Furthermore the energy of all charged particles excluding one of the  $\mu$  should be less than the beam energy. Since this condition is not fulfilled, this possibility can be rejected.

- Similar arguments rule out the production of spin one half charged heavy leptons  $L^\pm$ .

- The event topology can be explained by the production of a pair of heavy muons  $\mu^*$  decaying into  $\mu$  + hadrons. However, even with the assumption that the observed event is produced at threshold, about 30 such events would be expected for center of mass energies between 43.45 and 45.22 GeV using the cross section :

$$\sigma(e^+e^- \rightarrow \mu^+ \mu^{*-}) = \frac{2\pi}{3s} \beta(3-\beta^2) \quad \text{with } \beta = \left(1 - \frac{4M_{\mu^*}^2}{s}\right)$$

Another possibility would be to produce one  $\mu^*$  with  $e^+e^- \rightarrow \mu\mu^*$  for which unconventional currents of the form  $\frac{e}{\Lambda} \bar{\psi}_\mu \sigma^{\lambda\nu} F_{\lambda\nu} \psi_\mu$  [16] are needed ( $\Lambda$  is a scale parameter with mass dimension and  $F_{\lambda\nu} = \partial_\lambda A_\nu - \partial_\nu A_\lambda$ ).

The cross section for this process is :

$$\sigma = \frac{16\pi\alpha^2}{3\Lambda^2} \left(1 - \frac{M_{\mu^*}^2}{s}\right)^2 \left(1 + \frac{2M_{\mu^*}^2}{s}\right)$$

with a scale parameter of the order of 800 GeV, one event is expected for a  $\mu^*$  mass around 29 GeV/c<sup>2</sup> as suggested by both  $\mu^+$  + hadrons or  $\mu^-$  + hadrons combinations.

### γ) Heavy neutral particles

- The cross section for heavy neutrino production can be written :

$$\sigma(e^+e^- \rightarrow \nu_H \bar{\nu}_H) = \frac{G^2}{96\pi} \frac{s M_Z^4}{(s - M_Z^2)^2} \beta(3 + \beta^2) [1 - 4\sin^2\theta_W + 8\sin^4\theta_W]$$

with  $G$  the fermi constant,  $M_Z$  the  $Z^0$  mass and  $\theta_W$  the Weinberg angle. A  $20 \text{ GeV}/c^2$  neutrino pair produced has a cross section of  $0.3 \text{ pb}$  (i.e. 1.2 events are expected). In this case there would be no severe constraint on the mixing angles ( $\sum_\ell |U_{\ell H}|^2 > 9 \cdot 10^{-9}$  for a lifetime of  $10^{-10} \text{ s}$  for the heavy neutrino). This is obtained by expressing the lifetime  $\tau_H$  as a function of the  $\mu$  lifetime  $\tau_\mu$ ,  $M_\mu$  and  $M_H$  the  $\mu$  and  $H$  masses,  $\text{Br}(W \rightarrow e\nu_e)$  the branching ratio of the virtual  $W$  to electron ( $\approx .1$ ) and the element of the lepton mixing matrix :

$$\tau_H = \tau_\mu \left(\frac{M_\mu}{M_H}\right)^5 \text{Br}(W \rightarrow e\nu) \frac{1}{\sum_\ell |U_{\ell H}|^2}$$

However using a V-A coupling, the mass recoiling against the muon should have an average value around  $M_H/2$ . The observed jet masses are substantially lower than this value.

- Production of a pair of spin 0 heavy muonic neutrinos has been considered. The rate would be small for a  $20 \text{ GeV}/c^2$  scalar neutrino, essentially because of the  $\beta^3$  threshold behaviour (.12 event expected). It is also not clear that the observed event would fit in the phenomenological framework describing the decay of these objects [17].

### Conclusion

- No scalar boson decaying to  $e^+e^-$ ,  $\mu^+\mu^-$ ,  $\tau^+\tau^-$ ,  $\gamma\gamma$  has been observed at CELLO in the energy range between 39.79 and 45.22 GeV. A  $50 \text{ GeV}/c^2$  spin 0 particle can be ruled out provided the coupling constant  $a_H$  is greater than  $1.5 \cdot 10^{-4}$ .

- We have found one multihadronic event with 2 isolated energetic muons. Both the di-muon and the hadronic masses are large. We expect of the order of  $10^{-3}$  events of this kind from conventional sources.

## REFERENCES

- [1] CELLO Collaboration, H.J. Behrend et al.,  
Physica Scripta 23 (1981) 610.
- [2] UA1 Collaboration, G. Arnison et al., Phys. Letters 135B (1984) 250.  
UA2 Collaboration, P. Bagnaia et al., Phys. Letters 129B (1983) 130.
- [3] U. Baur, H. Fritzsch, H. Faissner, Phys. Letters 135B (1984) 313.  
F.W. Bopp et al., Preprints SI-83-24(1983), SI-84-3(1984).  
W. Hollik, B. Schrempp, F. Schrempp, DESY Report 84-011 (1984),  
R.D. Peccei, Preprint MPI-PAE/PTH 80/83 (1983).  
F.M. Renard, Preprint PM/83/11 (1983).
- [5] G. 't Hooft, in Recent Developments in Gauge Theories, Proceedings  
NATO Advanced Study Institute, Cargèse 1979 (Plenum, NY)p.135.
- [6] See Ref.[4] W. Hollik, B. Schrempp, F. Schrempp.
- [7] F.M. Renard, private communication.
- [8] B. Anderson, G. Gustafson, T. Sjostrand, Phys. Letters 94B (1980) 211.
- [9] C. Petersen et al., Phys. Rev. D27 (1983) 105.
- [10] W. Baciano et al., Phys. Rev. Letters 43 (1979) 1073.  
K. Chadwick et al., Phys. Rev. D27 (1983) 475.
- [11] CELLO Collaboration, H.J. Behrend et al., Z. Phys. C19 (1983) 291.
- [12] TASSO Collaboration, M. Althoff et al., DESY Report 83-121 (1983),  
to be published in Z. Physik.
- [13] H.G. Sanders, Thesis, RWTH Aachen Report HEP 74-07 (1974).
- [14] A. Klarsfeld, Thèse 3ème cycle, Orsay LAL 82/10 (1982).
- [15] F.A. Behrends, R. Kleiss, Nucl. Physics B177 (1981) 237.
- [16] G. Feinberg, Phys. Rev. D110 (1958) 1482.
- [17] R.M. Barnett et al., Phys. Rev. Letters 51 (1983) 176.

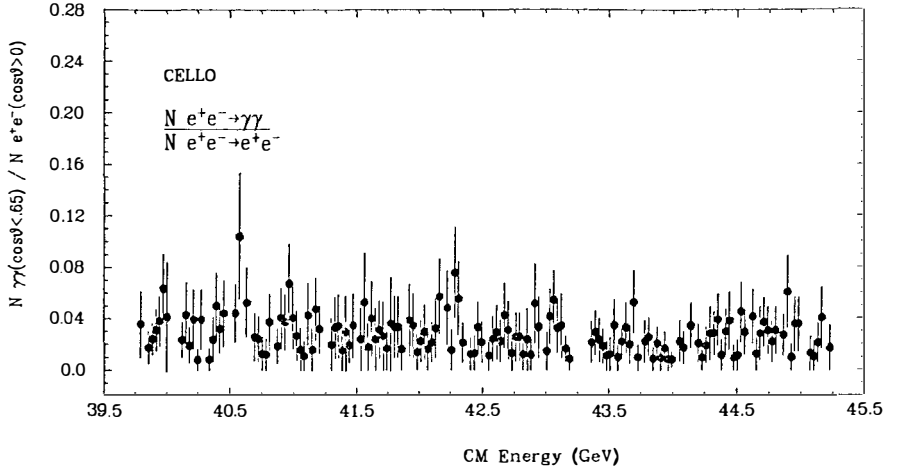


Fig. 1 - Ratio  $\sigma(e^+e^- \rightarrow \gamma\gamma)/\sigma(e^+e^- \rightarrow e^+e^-)$  in the energy span from 39.79 GeV to 45.22 GeV. ( $|\cos\theta_\gamma| < .65$  for  $e^+e^- \rightarrow \gamma\gamma$  and  $\cos\theta_e > .0$  for  $e^+e^- \rightarrow e^+e^-$ ).

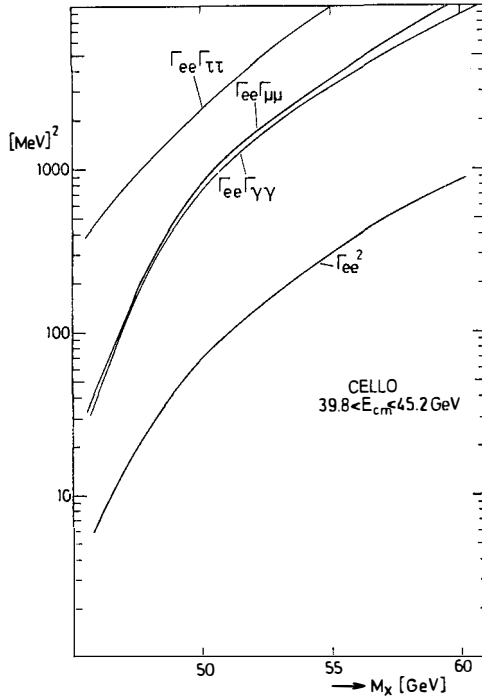


Fig. 2 - Upper limits at 95% CL for the product of the partial widths  $\epsilon\Gamma_{ee}\Gamma_{ii}$  ( $ii = e^+e^-, \mu^+\mu^-, \tau^+\tau^-, \gamma\gamma$ ) as a function of the mass  $M_X$  of the spin 0 boson.

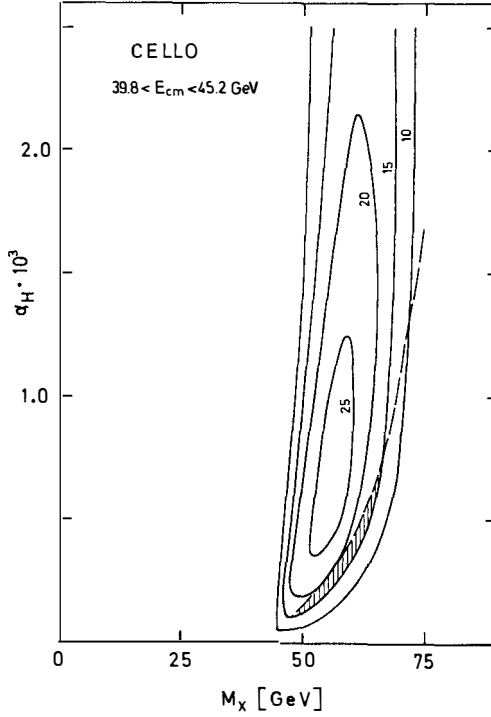


Fig. 3 - Limits at 95% CL for the coupling constant  $\alpha_H$  as a function of the scalar boson mass  $M_X$  from fits to the differential cross sections  $e^+e^- \rightarrow e^+e^-$  (dashed line) and  $e^+e^- \rightarrow \gamma\gamma$  (solid contours for different values of the radiative width  $\Gamma_R = \Gamma(Z \rightarrow X\gamma)$  in MeV). The hatched area shows the region allowed by the data for  $\Gamma_R > 15 \text{ MeV}$  and  $\epsilon = 1$ .



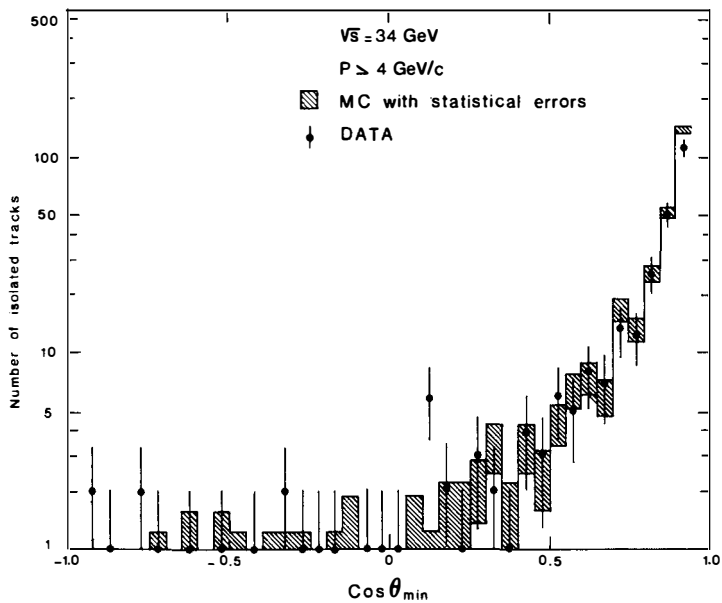


Fig. 5 - A comparison of Monte Carlo and data for the distribution of  $\cos \theta_{\min}$  at 34 GeV c.m. energy for hadrons with  $P > 4 \text{ GeV/c}$  ( $\theta_{\min}$  is the angle between the direction of the energetic track and the direction of the nearest charged particle).

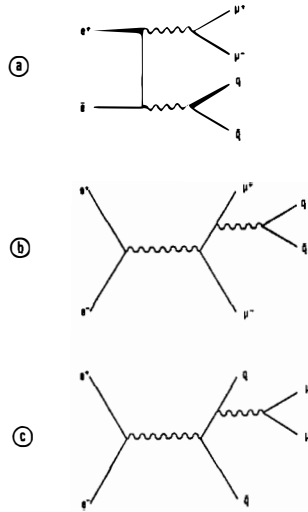


Fig. 6 - Feynman graphs for  $e^+e^- \rightarrow qq\mu^+\mu^-$  for order  $\alpha^4$ .

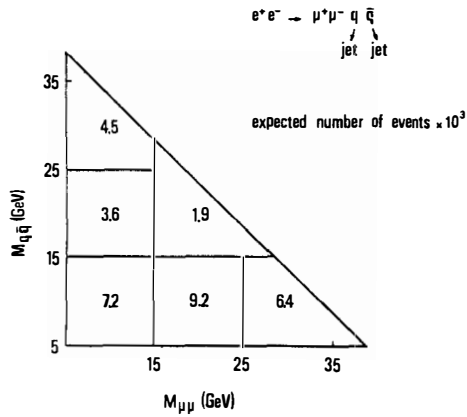


Fig. 7 - Number of expected events ( $\times 10^3$ ) for  $e^+e^- \rightarrow q\bar{q}\mu^+\mu^-$  process within acceptance and selection criteria as a function of  $\mu^+\mu^-$  and  $q\bar{q}$  masses estimated from diagrams in fig. 6.